Molecular Neurobiology (2019) 56:8364–8375
https://doi.org/10.1007/s12035-019-01684-9

Chronic Dyrk1 Inhibition Delays the Onset of AD-Like Pathology in 3xTg-AD Mice

R. Velazquez[1] · B. Meechoovet[2] · A. Ow[1] · C. Foley[3] · A. Shaw[3] · B. Smith[3] · S. Oddo[1,4] · C. Hulme[3] · Travis Dunckley[1]

Received: 17 May 2019 / Accepted: 17 June 2019 / Published online: 25 June 2019

Abstract

There is a critical need for new treatment approaches that can slow or prevent the progression of Alzheimer's disease (AD). Targets that act simultaneously on multiple relevant pathways could have significant therapeutic potential. Dual-specificity tyrosine phosphorylation-regulated kinase 1A (Dyrk1a) phosphorylates both amyloid precursor protein (APP) and tau. Dyrk1a is upregulated in post-mortem brains of AD patients, and such elevated expression is associated with cognitive deficits. We previously demonstrated that small molecule inhibition of Dyrk1 is well-tolerated and reduces amyloid plaques and pathological forms of tau in 3xTg-AD mice if administered after formation of these pathologies. However, while insoluble forms of hyperphosphorylated tau were reduced by Dyrk1 inhibition, overt neurofibrillary tangle (NFT) pathology remained unchanged. Herein, we specifically test the hypothesis that inhibition of Dyrk1 prior to NFT formation will delay the onset of pathology. 3xTg-AD mice were treated chronically, beginning at 6 months of age, prior to NFT pathology. Mice were dosed daily for either 3 or 6 months and amyloid and tau pathology were assessed. We show that chronic Dyrk1 inhibition reduces insoluble forms of amyloid beta peptides (Aβ) and hyper-phosphorylated tau long-term and that these reductions are associated with dramatic delay in the onset of both amyloid plaques and NFTs. In addition, we show that DYR219, a potent and selective small molecule Dyrk1 inhibitor, induces degradation of Dyrk1a protein, likely contributing to the efficacy of this small molecule approach in vivo. Collectively, these results suggest that therapeutic strategies targeting tau phosphorylation will show the greatest effect if administered very early in the pathogenesis of AD.

Keywords Alzheimer's disease · DYRK1A · Tau · Amyloid · 3xTg-AD · Therapeutics

Introduction

Targeting Alzheimer's disease (AD) pathology at single components is not likely to be feasible and a successful therapeutic strategy will require pleiotropic interventions [1–4]. Dual-specificity tyrosine phosphorylation-regulated kinase 1A (Dyrk1a) is an emerging target for the treatment of neurodegenerative diseases [5], attractive for its functional activity on multiple pathways implicated in AD and neuronal function. The Dyrk1a gene is located within the Down syndrome (DS) critical region on chromosome 21 and overexpression is a significant contributor to the underlying neurodevelopmental and AD-related abnormalities associated with DS [6–11]. Transgenic animals overexpressing Dyrk1a show marked cognitive deficits and impairment in hippocampal-dependent memory tasks [7, 8, 12].

In addition to its function in neuronal development, recent evidence has implicated Dyrk1a in the pathology of neurodegenerative disorders such as AD, dementia with Lewy bodies, and Parkinson's disease [13]. Dyrk1a has been shown to promote the formation of the pathological hallmarks of these diseases via hyperphosphorylation of their most abundant components, such as tau in neurofibrillary tangles (NFTs) [6, 9–11], amyloid-β precursor protein (APP) [7, 14], and α-synuclein in Lewy bodies [15]. The protein levels, as well as

C. Hulme and Travis Dunckley contributed equally to this work.

Electronic supplementary material The online version of this article (https://doi.org/10.1007/s12035-019-01684-9) contains supplementary material, which is available to authorized users.

✉ Travis Dunckley
Travis.Dunckley@gmail.com

[1] Neurodegenerative Disease Research Center, Biodesign Institute, Arizona State University, Tempe, AZ 85281, USA

[2] Neurogenomics Division, Translational Genomics Research Institute, Phoenix, AZ 85004, USA

[3] Division of Drug Discovery and Development, Department of Pharmacology and Toxicology, College of Pharmacy, The University of Arizona, Tucson, AZ 85721, USA

[4] School of Life Sciences, Arizona State University, Tempe, AZ 85281, USA

the catalytic activity of Dyrk1a, are increased in cortical neurons in both DS and AD [10, 16, 17]. Increased Dyrk1a immunoreactivity has been reported in the cytoplasm and nuclei of scattered neurons of the entorhinal cortex, hippocampus, and neocortex in neurodegenerative diseases associated with tau phosphorylation, including AD, DS, and Pick's disease [9]. These findings coupled with the observation that Dyrk1a inhibition can reduce tau hyperphosphorylation and rescue cognitive deficits in mouse models of DS [10, 18] and AD [19] indicate that Dyrk1a is a promising therapeutic target to treat these disorders.

The hyperphosphorylation of the microtubule-stabilizing protein tau contributes to the aggregation into NFTs, which are highly correlated with dementia severity in AD [20]. We and others have shown that Dyrk1a is important for phosphorylation of the tau protein on multiple sites [5, 6, 11, 21]. Phosphorylation of tau with Dyrk1a primes further tau phosphorylation by glycogen synthase kinase 3β (GSK-3β) [10]. Inhibition of Dyrk1a is thus expected to reduce abnormal tau phosphorylation with additive reduction of tau phosphorylation by GSK-3β, thereby possibly acting at two critical kinase pathways with synergistic protection against tau hyperphosphorylation and toxicity. Dyrk1a has also been shown to phosphorylate the amyloid precursor protein (APP) at Thr668, resulting in increased amyloidogenic cleavage of APP and elevated $A\beta_{40}$ and $A\beta_{42}$ levels, exacerbating β-amyloidosis [6, 14, 22]. In turn, Aβ oligomers are known to activate Dyrk1a [21]. Thus, inhibition of Dyrk1a may synergistically reduce the formation of Aβ oligomers through inhibition of APP phosphorylation via the Dyrk1a pathway [22]. Tau hyperphosphorylation is also induced by Aβ oligomers [23, 24]. Inhibition of Dyrk1a may thus additionally reduce the formation of NFTs via reduction of Aβ oligomer levels. Indeed, we recently demonstrated that inhibition of Dyrk1a, when pathology is advanced in the 3xTg-AD mouse model, reduces AD-like amyloid and tau pathology and improves cognition [19], consistent with the demonstrated roles for Dyrk1a in APP phosphorylation, Aβ production, and tau hyperphosphorylation.

Herein, we extend prior studies to demonstrate that Dyrk1 inhibition prior to the onset of AD-like pathology in 3xTg-AD mice significantly delays the onset of both amyloid and tau pathologies. We also confirm that a relatively rare mechanism of action, based on inhibitor-induced degradation of Dyrk1a protein, likely contributes to the beneficial effects seen on AD-like neuropathology that result from inhibition of Dyrk1 with type I kinase inhibitors.

Results

DYR219 Is a Potent and Selective Dyrk1 Inhibitor

DYR219 is a benzimidazole analog (Patent #US2016/050198) that functions as a type 1 ATP-competitive kinase inhibitor [19] and through a rarely seen protein degradation mechanism not initiated by proteolysis-targeting chimeras (PROTACS) [25]. DYR219 was developed via a knowledge-based approach using co-crystal structures of harmine, D15, and Indy bound to Dyrk1a (PDB ref# 3ANQ, 2WO6, and 3ANR, respectively). Hybrid structures of these three early inhibitors were synthesized to afford low micromolar inhibitors and subsequent optimization gave DYR219. Using in vitro phosphorylation assays ([ATP] 45 μM) with synthetic peptide substrates, DYR219 inhibited Dyrk1a activity with an IC_{50} of 34 nM. Like the majority of Dyrk1a inhibitors reported to date, DYR219 proved equipotent with Dyrk1b (IC_{50} 29 nM). It possessed only nominal activity versus two major tau kinases GSK3β (34% at 20 μM) and CDK5 (55% at 20 μM). To assess broader kinase selectivity, a KinomeScan™ (468 panel: https://www.discoverx.com) was performed at the relatively high concentration of 10 μM for DYR219 (K_D 16 nM). The S(35)-selectivity score was 0.19 (Fig. 1), which is comparable with marketed kinase inhibitors (K_D Dyrk1a 16 nM). In in vitro phosphorylation assays using full-length recombinant tau protein, DYR219 inhibited Dyrk1a catalyzed tau phosphorylation at the pS396 epitope (IC_{50} = 127 nM; [ATP] = 1 mM) (Fig. 2a). In H4 neuroglioma cells expressing 4R0N tau [11, 26], DYR219 inhibited tau protein phosphorylation at the pS396 epitope with an EC_{50} of 142 nM (Fig. 2b).

DYR219 had a favorable cytotoxicity profile, reducing phospho-tau (and total tau) well before detection of cytotoxicity (> 95% viability at EC_{50}) (Fig. 3). In pharmacokinetic studies wherein DYR219 was delivered via intra-peritoneal (IP) injection (12.5 mg/kg), DYR219 readily crossed the BBB [brain: DYR219 C_{max} 344 ng/ml (1.05 μM at 15 min)] and was cleared within ~ 1–3 h (Fig. 4, Supplementary Table 1). These combined results indicated that DYR219 was a potent, brain-penetrant, and selective Dyrk1 inhibitor worthy of evaluation in an in vivo setting of AD.

Dyrk1 Inhibition Reduces Tau Pathology in 3xTg-AD Mice

We previously demonstrated that treatment of 10-month-old 3xTg-AD mice with DYR219 after the mice had already developed neurofibrillary tangle (NFT) pathology significantly improved memory and reduced accumulation of insoluble, hyperphosphorylated tau protein [19]. However, in that prior study, we observed no changes in overt NFT pathology. Herein, we tested the hypothesis that the DYR219 inhibitor would delay the onset of NFT pathology when Dyrk1 was inhibited prior to formation of NFT pathology. To do this, we treated 6-month-old 3xTg-AD mice prior to NFT pathology onset (Fig. 5). Mice were treated with either DYR219 via once daily IP injection (12.5 mg/kg) or vehicle. Both DYR219- and vehicle-treated groups were separated into two cohorts. One cohort received treatment for 3 months (pathology assessed at 9 months of age;

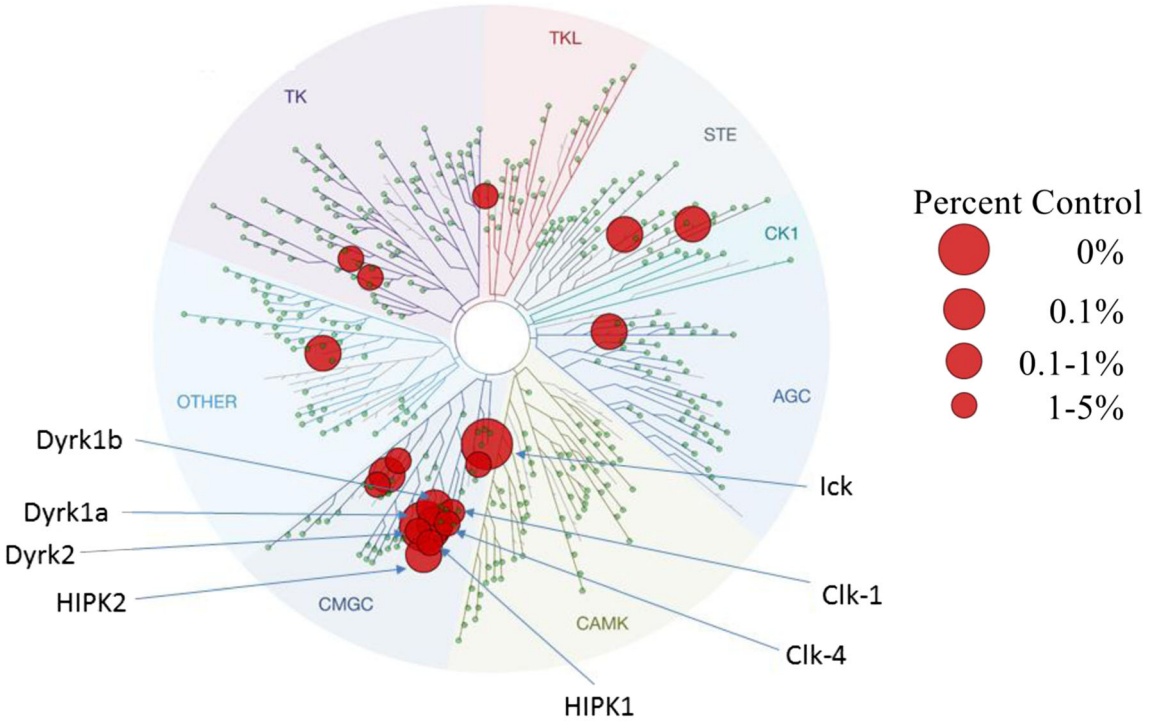

Fig. 1 KinomeScan™ was performed against 468 kinases using 10 μM DYR219. The side legend correlates circle size to % activity relative to control. Additional data shown include IC_{50} values against Dyrk1b and % inhibition of GSK3β and CDK5 at 20 μM. Select targets in the CMGC kinase family are indicated

$N = 10$ mice per vehicle and DYR219 groups) and the second cohort was treated for 6 months (pathology assessed at 12 months of age; $N = 10$ mice per vehicle and DYR219 groups).

To determine if DYR219 could delay NFT pathology onset, we performed immunohistochemistry on hippocampal sections of 3xTg-AD mice using the AT8 phospho-tau antibody. Results demonstrated a significant delay in the onset of NFT pathology (Fig. 6a). At 9 months of age, following 3 months of DYR219 administration, vehicle-treated mice developed NFT pathology as expected. In contrast, all 10 DYR219-treated mice had no detectable NFT pathology. In the 12-month cohort, vehicle-treated mice had abundant NFT pathology. In the DYR219-treated group, NFT pathology was significantly reduced. Indeed, 6 mice had no detectable NFT pathology at all and only a handful of NFTs could be identified in the remaining mice. This dramatic reduction in NFT pathology was accompanied by significant reductions in insoluble, hyperphosphorylated tau protein (Fig. 6b), as assessed by western blot for pS396 tau ($p = 0.0024$ at 9 months; $p = 0.014$ at 12 months). Levels of soluble phosphorylated forms of tau protein were unaffected (data not shown), similar to what was observed previously [19]. Insoluble total tau protein was also significantly reduced in the 3-month treatment group ($p = 0.0036$). There was a trend toward reduced total tau protein following 6 months of DYR219 treatment ($p = 0.092$). However, while all treatment groups showed greater reductions to phosphorylated tau levels relative to total tau levels, DYR219 promoted tau degradation in cell culture (see below).

Dyrk1 Inhibition Reduces Amyloid Pathology in 3xTg-AD Mice

In addition to tau pathology, 3xTg-AD mice show age-dependent amyloid pathology by 9 months of age [27]. To determine effects of DYR219 on amyloid pathology, we immunostained hippocampus containing sections with an $A\beta_{42}$-

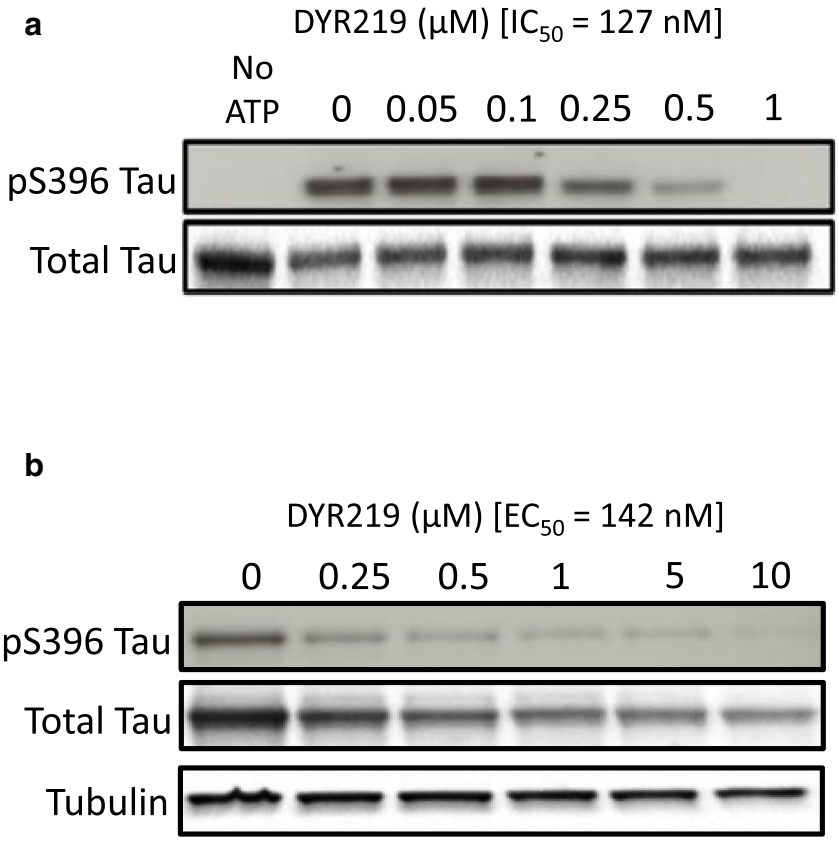

Fig. 2 DYR219 is a potent Dyrk1a inhibitor. Shown in **a**, in vitro phosphorylation results using recombinant Dyrk1a and tau proteins and the indicated concentrations of DYR219. Assays were performed per the "Materials and Methods" section. The IC_{50} was 127 nM. In **b**, results from a cell-based assay of DYR219 effects on pS396 tau and total tau. The assay has been described previously in detail [26]. The EC_{50} was 142 nM for pS396 tau

specific antibody. Remarkably, we found that DYR219 mice had no detectable amyloid pathology at 9 months of age, in sharp contrast to the substantial amyloid pathology observed in vehicle-treated mice (Fig. 7a). At 12 months of age, DYR219-treated 3xTg-AD mice began to develop amyloid pathology, but at drastically reduced levels compared to

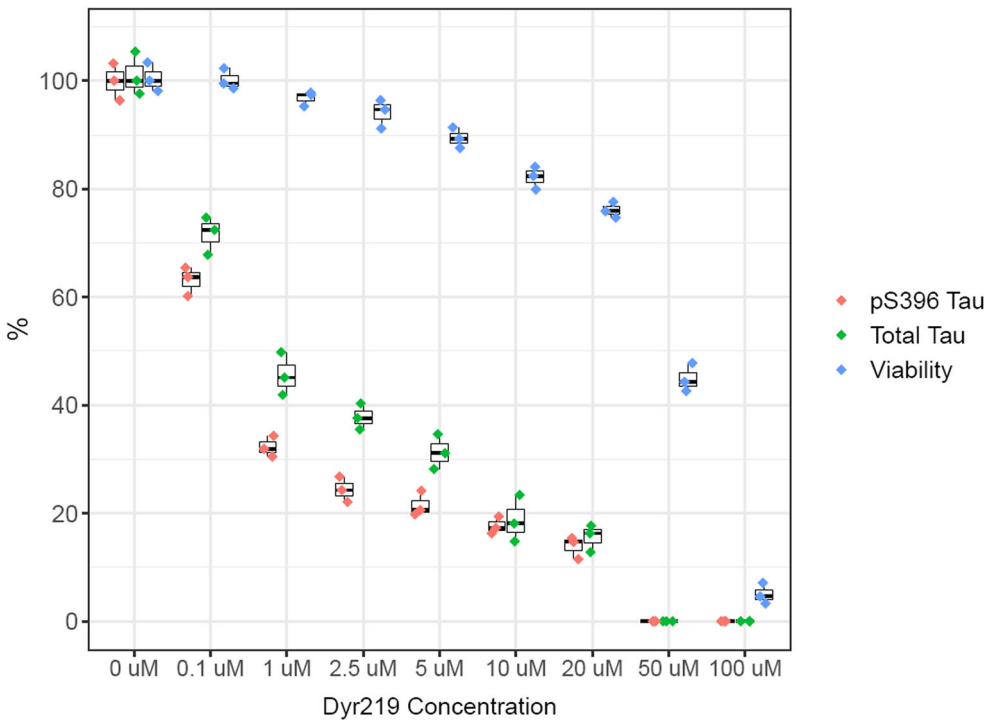

Fig. 3 DYR219 reduces pS396 tau before any significant cytotoxicity. Shown are graphs of results from westerns assessing levels of pS396 tau and total tau overlayed with MTT toxicity assay results for the indicated concentrations of DYR219. Viability is > 95% at the EC_{50} concentration of DYR219. Error bars are standard deviation ($n = 3$ per each concentration tested). Importantly, for visualization purposes, points are not directly overlayed above each concentration. However, the concentrations along the *x*-axis are the concentrations at which pS396 tau, total tau, and viability were assessed

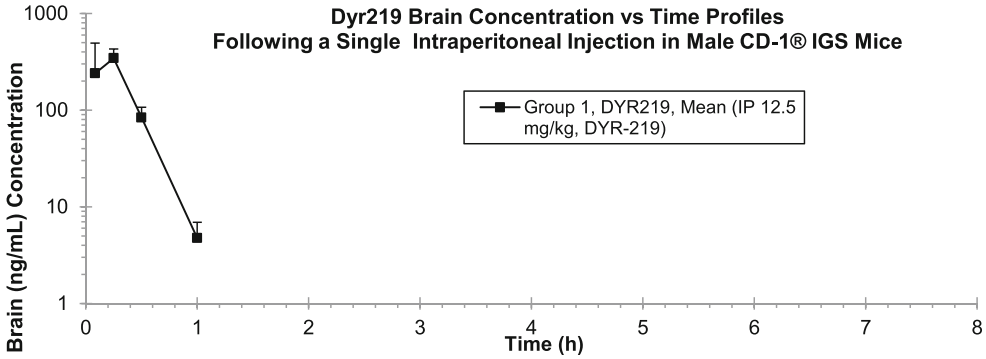

Fig. 4 Pharmacokinetic profile of DYR219. Brain exposure (ng/ml) is plotted at the indicated times (*x*-axis) following a single intra-peritoneal injection at 12.5 mg/kg ($n = 3$ mice per time point)

vehicle-treated mice. Quantitative analysis of plaque load (Fig. 7b) showed these results to be highly statistically significant ($p = 7.9E\text{-}05$ at 9 months; $p = 5.2E\text{-}05$ at 12 months). Reductions to amyloid plaque burden were accompanied by significant reductions to insoluble forms of $A\beta_{42}$ and $A\beta_{40}$ peptides, as assessed by ELISA ($p = 0.0076$ at 9 months; $p = 0.0029$ at 12 months) (Fig. 7c). Consistent with our prior observations [19], we observed no differences in soluble Aβ peptides in any treatment group (data not shown). We previously demonstrated that these changes to amyloid pathology and Aβ peptides are associated with reduced amyloid precursor protein (APP) phosphorylation and increased lysosomal degradation of full-length APP [19].

DYR219 Promotes Dyrk1a Degradation Via the Proteasome

DYR219 rapidly enters the brain following IP administration (Fig. 4). However, DYR219 is subsequently cleared from the brain within 2 h. An obvious question is how the robust neuropathological effects, observed both herein and previously [19], can be achieved by relatively modest exposure. Dyrk1a is a dual-specificity kinase, undergoing autocatalytic tyrosine phosphorylations during synthesis of the protein [28]. It has recently been discovered that type I inhibitors acting on Dyrk1a also inhibit this autophosphorylation event, preventing the formation of mature and active Dyrk1a while

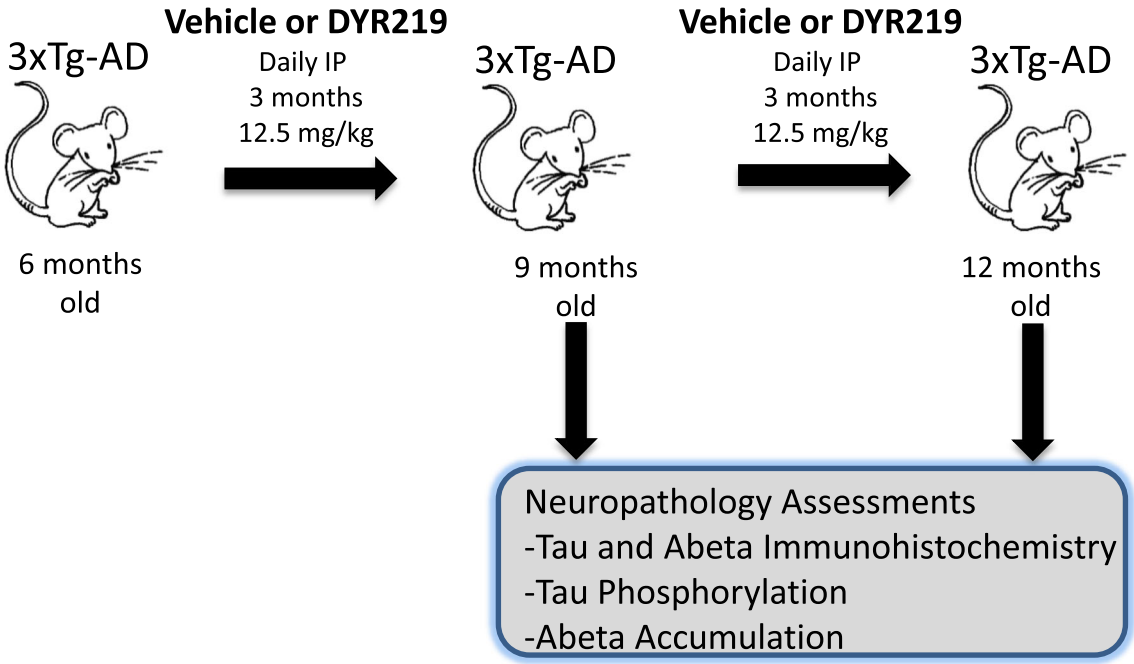

Fig. 5 Schematic representation of the study design. Six-month-old 3xTg-AD mice were dosed once daily for either 3 months or 6 months with DYR219 or vehicle. Following each dosing period, $n = 10$ mice per vehicle and DYR219 group were sacrificed and neuropathology assessed as described in the text

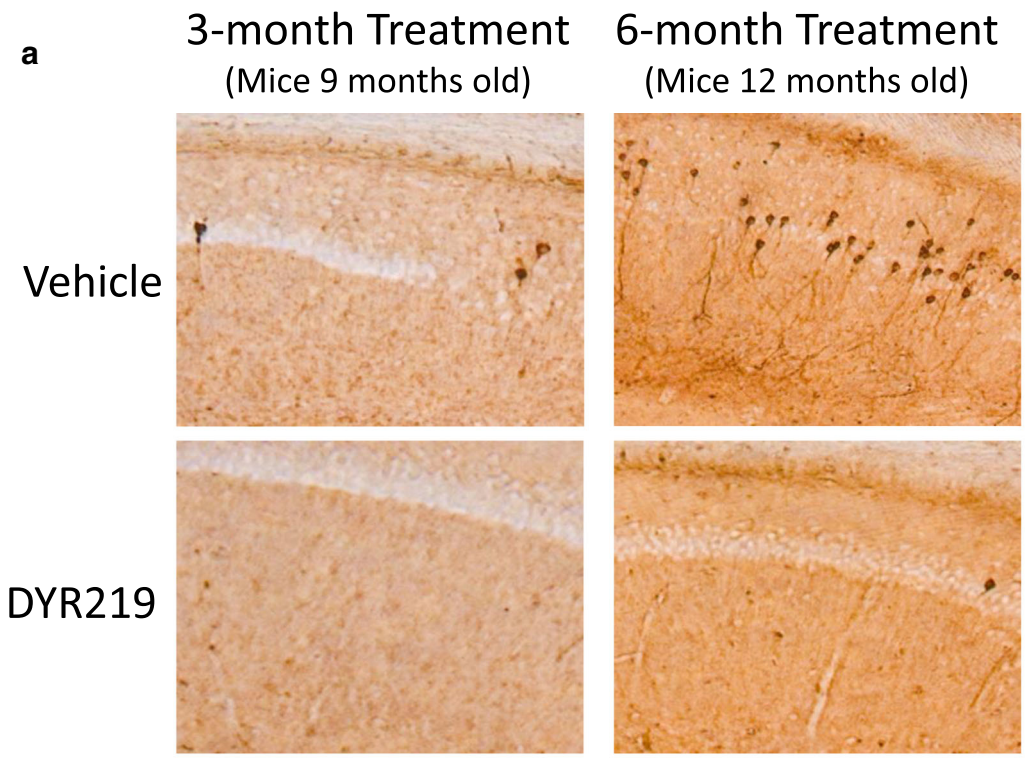
a
3-month Treatment
(Mice 9 months old)
6-month Treatment
(Mice 12 months old)
Vehicle
DYR219

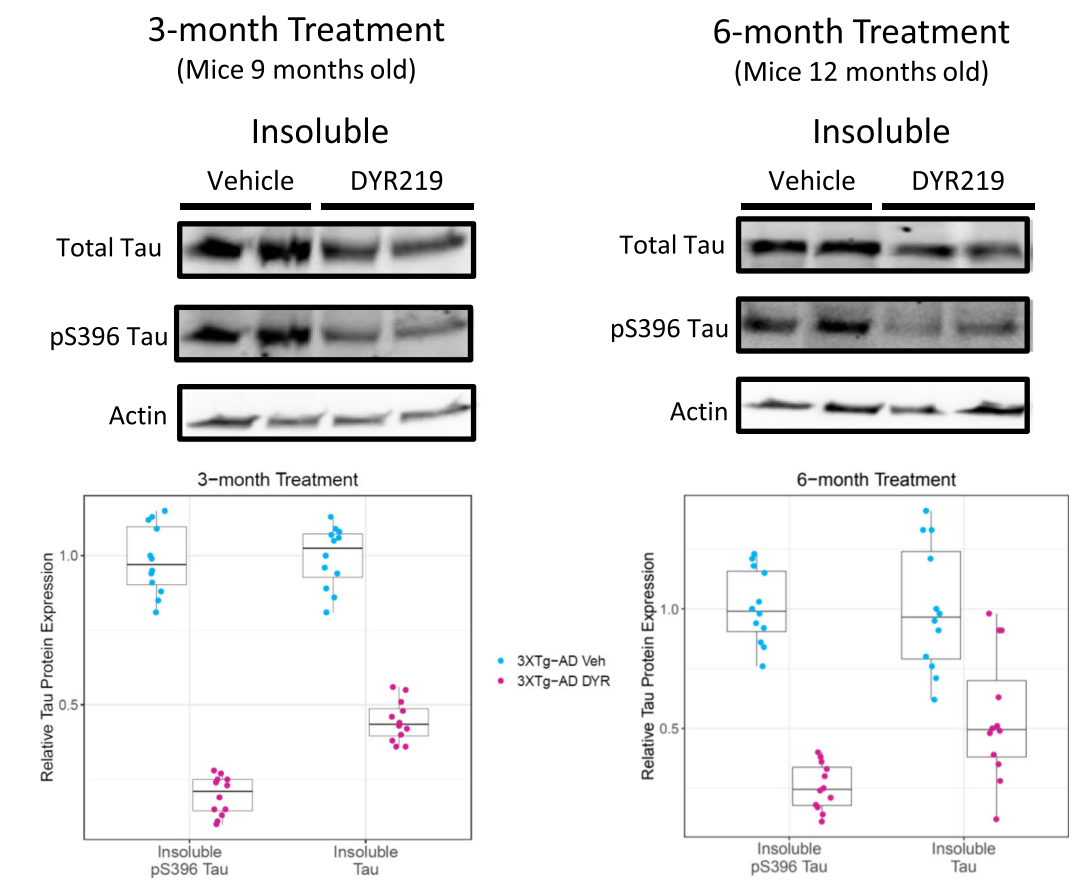
b
3-month Treatment
(Mice 9 months old)
Insoluble
Vehicle
DYR219
Total Tau
pS396 Tau
Actin
6-month Treatment
(Mice 12 months old)
Insoluble
Vehicle
DYR219
Total Tau
pS396 Tau
Actin
3−month Treatment
6−month Treatment
Relative Tau Protein Expression
1.0
0.5
3XTg−AD Veh
3XTg−AD DYR
Insoluble pS396 Tau
Insoluble Tau

◀ **Fig. 6** DYR219 delays tau pathology in 3xTg-AD mice. Shown in **a**, representative immunohistochemistry images from vehicle- and DYR219-treated mice at age 9 months and 12 months. No DYR219 mice had any neurofibrillary tangles after 3 months of treatment. Half of the 12 mice were completely clear after 6 months of daily dosing. Shown in **b**, western results of pS396 tau and total tau in the insoluble protein fraction from vehicle- and DYR219-treated mice. Bar graphs represent quantitation of westerns for all mice ($N = 10$) per group. Error bars are standard deviation

also promoting degradation of the protein [29]. This appears to be a generalizable feature of Dyrk1a type I ATP-competitive kinase inhibitors, with the well-established inhibitors harmine, INDY, and CaNDY all showing this effect [29]. To potentially explain the apparent pharmacodynamic/pharmacokinetic mismatch of DYR219, we sought to determine if DYR219 could also be promoting the degradation of Dyrk1a protein. To do this, we first treated H4 neuroglioma cells expressing the 4R0N tau isoform (first described in Azorsa et al. [11]) with escalating concentrations of DYR219 and measured pS396 tau, total tau, and full-length Dyrk1a protein levels via western. We observed the expected reductions to pS396 tau ($EC_{50} = 134$ nM) and total tau ($EC_{50} = 356$ nM) that have previously been observed for a broad range of Dyrk1a inhibitors (Fig. 8a) [26]. However, we also observed a significant dose-dependent reduction in Dyrk1a protein levels ($EC_{50} = 625$ nM), consistent with DYR219 promoting degradation of Dyrk1a. We next treated H4-Tau cells with 5 μM DYR219 in the presence or absence of MG-132 (5 μM), a potent proteasome inhibitor. Following 24 h of treatment, we observed consistent reductions to pS396 phosphorylated tau levels regardless of proteasome inhibition (Fig. 8b). However, we found that the reductions to both total tau and Dyrk1a proteins were dependent upon proteasome function, as MG-132 prevented reductions to both proteins in the presence of DYR219. Lastly, we performed Dyrk1a westerns using cortical tissue from the 3-month and 6-month DYR219-treated 3xTg-AD mice and found significant reductions in steady-state Dyrk1A protein levels at both treatment time points (Fig. 8c). These combined results indicate that DYR219 promotes degradation of Dyrk1a protein and that this effect, seen in vivo, could contribute to the pronounced pharmacodynamic effects of this compound.

Discussion

Early Inhibition of Dyrk1 Delays Onset of AD-Like Pathologies

There are currently no therapeutic options to delay the onset or progression of Alzheimer's disease (AD). We report here results of an AD pathology prevention study in the 3xTg-AD mouse model using the novel Dyrk1a inhibitor, DYR219. DYR219 is the identical Dyrk1a inhibitor that we previously reported as dyrk-inh in Branca et al. [19]. However, herein, we extend prior findings to demonstrate that chronic Dyrk1 inhibition can significantly delay the onset of both amyloid and tau pathologies. The 3xTg-AD mouse model of AD generates age-dependent amyloid and tau pathologies [30] and, as such, provides a useful model for testing interventions that may delay onset or progression of both pathologies. To test whether Dyrk1 inhibition could delay pathology onset or progression, we treated 6-month-old 3xTg-AD mice with the Dyrk1 inhibitor, DYR219, for periods of up to 6 months via once daily IP injection. At 6 months of age, the 3xTg-AD mice have no neurofibrillary tau (NFT) pathology and minimal amyloid plaque pathology in the CA1 region of the hippocampus [30]. Following 3 months of DYR219 administration, all drug-treated 3xTg-AD mice were completely clear of both amyloid and tau neuropathologies, whereas vehicle-treated mice developed both pathologies. After 6 months, vehicle-treated mice accumulated large amounts of both amyloid plaque (Fig. 7) and NFT pathologies (Fig. 6) at 12 months of age, as expected [30]. By comparison, DYR219-treated mice showed significantly reductions in the amounts of both pathologies, which was matched by significant reductions in the main protein components of these neuropathologies.

In prior work testing DYR219 in 3xTg-AD mice [19], dosing was initiated at 10 months of age, a time point in which mice have developed substantial amyloid pathology and significant NFT pathology [30]. In those studies, DYR219 treatment significantly reduced amyloid plaque burden, but did not alter the number of NFT present in the CA1 region. Here we clearly demonstrate that, if Dyrk1 inhibitors are administered prior to NFT formation, the onset of subsequent NFT pathology can be significantly delayed. This suggests that therapies targeting tau hyperphosphorylation will likely show the greatest effect if administered very early in the disease process. Importantly, while we previously demonstrated significant cognitive improvements in the absence of reduced NFT pathology [19], we did not assess behavioral metrics in the current study. Thus, an outstanding question remains whether the improved neuropathological outcomes herein translate to improved cognitive outcomes as well.

In contrast to tau pathology, amyloid pathology can be reduced by Dyrk1 inhibition even if Dyrk1 is inhibited following the formation of amyloid plaques. Reasons for this distinction remain unclear. However, it is tempting to speculate that different mechanisms of clearance for each pathology could play an important role. Based on known effects of Dyrk1a activity in promoting Aβ peptide production [14, 21, 22] and tau hyperphosphorylation [10, 11, 26, 31], inhibition of Dyrk1a should slow the generation of Aβ plaques and NFT. In the case of amyloid plaques, subsequent clearance pathways, possibly mediated by microglia [32], could then reduce amyloid plaque burden. Mature tau pathology cannot

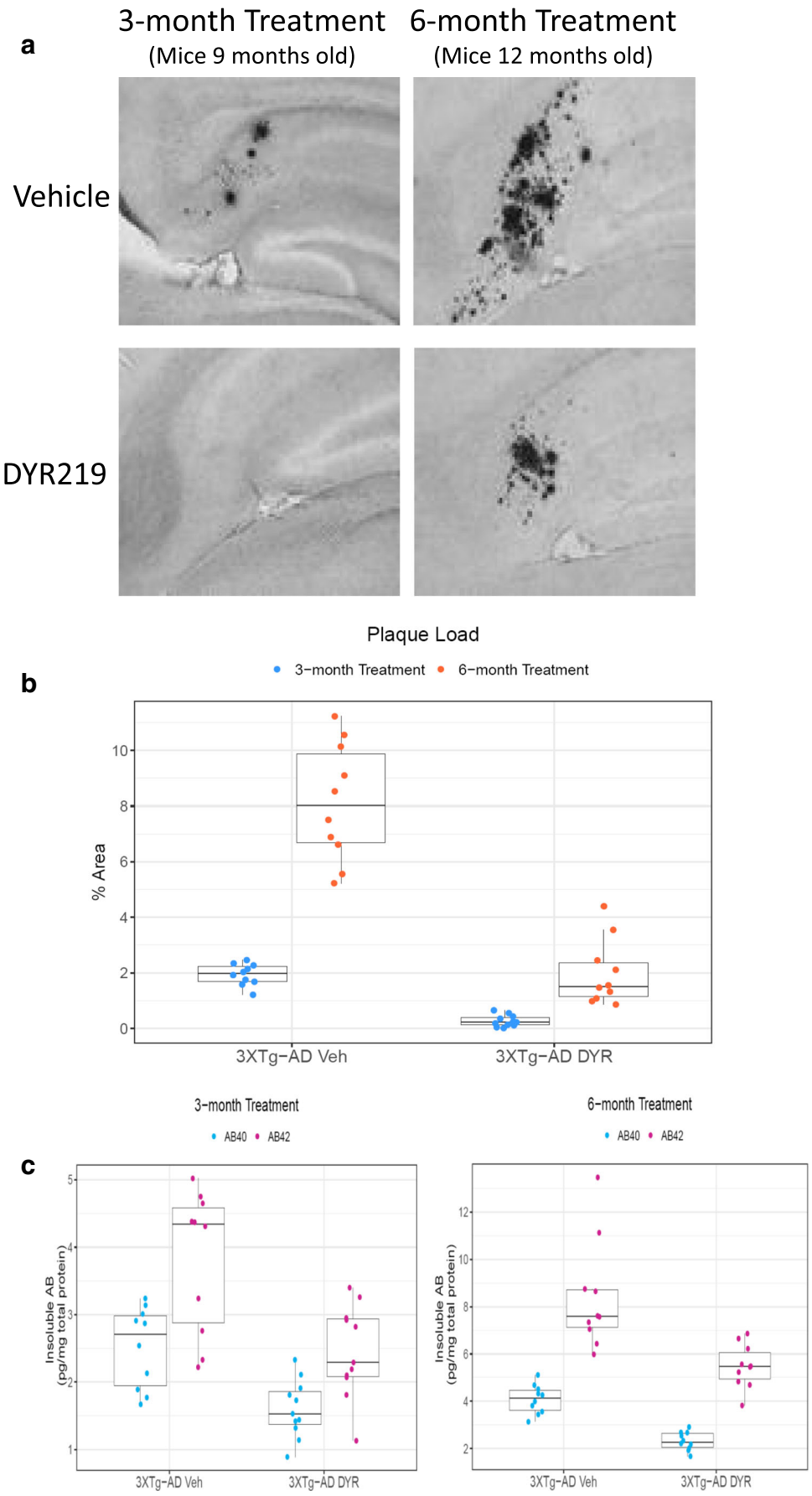
a
3-month Treatment
(Mice 9 months old)
6-month Treatment
(Mice 12 months old)
Vehicle
DYR219
b
Plaque Load
3−month Treatment
6−month Treatment
% Area
0
2
4
6
8
10
3XTg−AD Veh
3XTg−AD DYR
c
3-month Treatment
6-month Treatment
AB40
AB42
Insoluble AB
(pg/mg total protein)
3XTg-AD Veh
3XTg-AD DYR

◀ **Fig. 7** DYR219 delays amyloid pathology in 3xTg-AD mice. Shown in **a**, immunohistochemistry of amyloid plaques in vehicle- and DYR219-treated 3xTg-AD mice at the indicated ages. No DYR219-treated 3xTg-AD mice had any detectable amyloid plaques at 9 months of age. At 12 months of age, mice developed plaque pathology at levels lower than 9-month-old vehicle-treated mice. Quantitation of plaque load is shown in **b** ($n = 10$ mice per group). Shown in **c** are ELISA results for $A\beta_{42}$ and $A\beta_{40}$ from the insoluble protein fractions ($n = 10$ mice per group). Aβ peptides were significantly reduced in DYR219-treated mice at all time points

be cleared by Dyrk1 inhibition if administered after NFTs have already formed. This result is consistent with prior results in 3xTg-AD mice showing that Aβ immunotherapy approaches can reduce NFT pathology if administered early, but not late, in the progression of NFTs [33], a result analogous to what is observed here with Dyrk1 inhibition.

Degradation of Dyrk1A Likely Contributes to Beneficial Effects on AD Pathology

Some small molecule kinase inhibitors have been shown to induce protein degradation of kinases via the proteasome. These inhibitors have typically been discovered serendipitously, as opposed to being uncovered through rational design strategies. An example is seen for inhibitors of MELK (maternal embryonic leucine zipper kinase), which result in proteasomal degradation due to the postulated loss of autophosphorylation [34]. Conversely, there are a plethora of rationally designed small molecules with clinical applications that control intracellular protein levels through chemical knockdown. As such, targets of interest binding moieties are typically coupled to recognition motifs of E3 ligases. When dual target and ligase binding occurs, protein is shunted to the proteasome and degraded. This technology, known as proteolysis-targeting chimeric molecules (PROTACS) [35], is showing clinical promise. However, linker and ligase recognition motifs often confer physico-chemical properties that are detrimental to passive BBB penetration. As such, this raises the bar for PROTAC CNS drug discovery where managing appropriate physicochemical properties to enable brain exposure becomes more challenging for the medicinal chemist. The discovery that DYR219, devoid of a proteolysis targeting chimera, induces Dyrk1a degradation is thus a major advantage, which will likely reduce design burdens on type 1

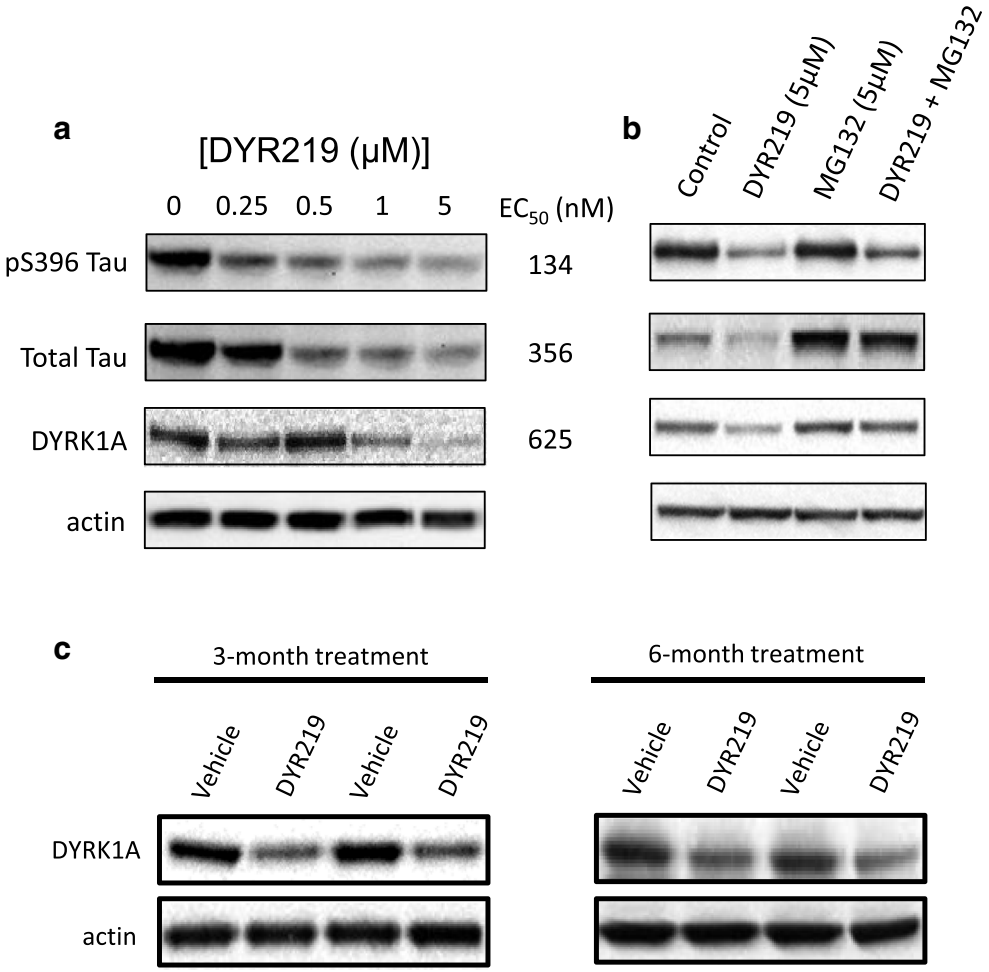

Fig. 8 DYR219 induces Dyrk1a protein degradation via the proteasome. Shown in **a**, pS396 tau, total tau, and Dyrk1a protein levels in H4-tau cells [26] at the indicated concentrations of DYR219. The EC_{50} against each protein is indicated. Shown in **b**, H4-tau cells treated with 5 μM DYR219 in the presence or absence of MG-132 (5 μM) to inhibit proteasome activity. Cells were treated for 24 h and pS396 tau, total tau, and Dyrk1a levels assessed. MG-132 prevented DYR219-induced reductions to total tau and Dyrk1a, but not pS396 tau. In **c**, cortical protein lysates from 3xTg-AD mice treated with vehicle or DYR219 for the indicated durations were analyzed for Dyrk1a expression via western. Dyrk1a expression was reduced at both 3-month and 6-month time points in DYR219-treated mice relative to vehicle controls

ATP-competitive selectivity within the kinome as, to date, only a small subset of kinases have been shown to be susceptible to inhibitor-induced degradation.

Materials and Methods

3xTg-AD Mice

Generation of the 3xTg-AD mice has been described previously [27]. In our colony of 3xTg-AD mice, the AD-like pathology in males is highly variable. However, the onset and progression of pathology in females is highly consistent and predictable [30]. Thus, this study used only female mice. All mice were housed 4–5 per cage on a 12-h light/dark cycle and provided food and water ad libitum. Animal care and treatments were in accordance with the applicable regulation of the vivarium (The Institutional Animal Care and Use Committee of the Arizona State University).

DYR219

DYR219 was synthesized by Dr. Hulme (University of Arizona) and confirmed > 99% pure by liquid chromatography. For chronic treatments, DYR219 was delivered via daily intraperitoneal (i.p.) injection at 12.5 mg/kg in 50% PEG-400 and 50% 0.9% NaCl. Control (vehicle) mice were treated with an equal volume of vehicle. Mice were weighed weekly.

In Vitro Tau Phosphorylation Assay

Tau in vitro phosphorylation assays have been published previously [26]. Evaluation of DYRK1A kinase activity was determined by incubating 0.08 μg of recombinant human Dyrk1a protein (Invitrogen) with 0.15 μg of 4R2N recombinant human tau (SignalChem) in 1X kinase buffer (25 mM Tris-HCl (pH 7.5), 5 mM beta-glycerophosphate, 2 mM dithiothreitol (DTT), 0.1 mM Na3VO4, 10 mM MgCl2—Cell Signal) and 1 mM ATP in a final volume of 20 μl for 30 min at 30 °C. The reaction was inactivated upon addition of 1X Novex LDS sample buffer and Novex sample reducing reagent, 50 mM DTT, (Invitrogen) followed immediately by heating for 10 min at 95 °C. Phosphorylated tau was resolved using 7% Tris-acetate gels and detected by western analysis. Westerns were probed for phospho-tau S396 (Abcam) at 1:5000 dilution and a secondary of goat anti-rabbit HRP (Jackson Immuno Labs) at 1:50,000 in 5% BSA. Membranes were stripped as above and reprobed with rabbit anti-human total tau (Dako) at 1:15,000 dilution and a secondary of goat anti-rabbit HRP (Jackson Immuno labs) at 1:100,000 dilution in 5% milk. β-Actin was used as a loading control to normalize proteins of interest.

Cellular Tau Assay

Details of the cellular phospho-tau assay have been published previously [26]. H4-Tau cells [11] were incubated with indicated concentrations of DYR219 for 96 h at 37 °C and 5% CO_2. For experiments of Fig. 8b, treatment duration was for only 24 h. For other treatments, every 24 h, culture medium was removed and fresh culture media and compound were added. Cell viability was determined using MTT assays (Abcam) per the manufacturer's protocol. For tau assays, cell lysates were prepared using the Complete Lysis-M, EDTA-free kit (Roche Applied Science) supplemented with phosphatase inhibitor cocktails 1 and 2 (Sigma). Lysates were quantified using the BCA protein assay (Pierce). Protein from lysates (30 mg total protein per lane) were separated on SDS-PAGE gels and transferred to nitrocellulose membrane. Membranes were blocked in 5% blocking solution for 1 h at room temperature (RT). Blocking buffer solution used for detection of non-phosphorylated protein contained 5% non-fat dry milk in 1X TBS-T (50 mM Tris-HCl pH 7.4, 137 mM NaCl2, 2.7 mM KCl, 0.1% Tween). For detection of phosphorylated protein, blocking buffer solution contained 5% bovine serum albumin in 1X TBS-T. Membranes were probed with primary antibody [anti-tau (1:2000 dilution; Dako), anti-pS396 tau (1:5000 dilution; Abcam), and anti-DYRK1A (1:500 dilution; Santa Cruz)] in blocking buffer overnight at 4 °C on a rocker. Membranes were subsequently washed with 1X TBS-T and probed with secondary antibody in blocking buffer for 45 min using a 1:25,000 dilution of HRP-GAM or HRP-GAR (Jackson Immunoresearch), depending on the species (mouse or rabbit) in which the primary antibodies were raised. Following incubation with secondary antibody, membranes were washed in 1X TBS-T and developed with Super Signal West Femto Maximum Sensitivity Substrate Kit (Promega) and digitally imaged. Protein band signal saturation was assessed before any further analysis of multiple forms of tau. Alpha Innotech Fluoro Chem SF imaging software verifies degrees of saturation when signal intensity is beyond the dynamic range (which is from 0 to 65,535). Protein band signal intensities used for quantification were within the instrument's dynamic range. To test multiple primary antibodies, membranes were stripped for 15 min at RT using ReBlot Plus Mild Antibody Stripping Solution (Millipore). Membranes were then washed for 5 min in 1X TBS-T and blocked for 1 h in 5% blocking solution at RT. For verification of protein loading, membranes were reprobed overnight at 4 °C with an anti-tubulin primary antibody (1:1000 dilution;

Cell Signaling) or anti-actin primary antibody (1:10,000 dilution; Abcam).

Protein Extractions from Brain Tissue

Mice were sacrificed by CO_2 asphyxiation. Brains were removed and sagittally bisected. Half of the brain was fixed in 4% paraformaldehyde and used for subsequent immunohistochemical experiments. The other half was collected and stored at − 80 °C until use. Frozen brains (without cerebellum) were processed as described previously [36]. Brains were homogenized in tissue protein extraction reagent (T-PER; ThermoFisher Scientific) containing 0.7 mg/ml of pepstatin A supplemented with a complete mini protease inhibitor tablet (Roche Applied Science) and phosphatase inhibitors (Millipore). The homogenates were centrifuged at 4 °C for 1 h at 100,000*g*, and the supernatant was stored as the soluble fraction. The pellet was homogenized in 70% formic acid and centrifuged as described above. The supernatant was stored as the insoluble fraction.

Western Blot and ELISA of Brain Extracts

Proteins from insoluble and soluble fractions were resolved by 10% Bis-Tris SDS-polyacrylamide gel electrophoresis (ThermoFisher Scientific) under reducing conditions and transferred to a nitrocellulose membrane. Membranes were developed as described above. Ab_{40} and Ab_{42} levels were determined with commercial ELISA kits (ThermoFisher Scientific) following the manufacturer's protocols.

Immunohistochemistry

Brains were processed as previously described [37]. Hemibrains were fixed in 4% paraformaldehyde in phosphate-buffered saline for 48 h and then transferred into 0.02% sodium azide in phosphate-buffered saline. Fifty-micrometer-thick free-floating sections were cut using a vibratome. For immunohistochemistry, sections were washed twice with TBS (100 mM Tris pH 7.4, 150 mM NaCl) and incubated for 30 min in 3% H_2O_2. Sections were washed in TBS-A (100 mM Tris pH 7.4, 150 mM NaCl, 0.1% Triton X-100) and TBS-B (100 mM Tris pH 7.4, 150 mM NaCl, 0.1% Triton X-100, 2% bovine serum albumin) for 15 and 30 min, respectively. Primary antibody was then applied overnight at 4 °C (AT8 1:1000 from ThermoFisher; 6E10 1:3000 from Cell Signaling Technology). Sections were washed and incubated in secondary antibody for 1 h at RT. Signal was enhanced by incubating sections in the avidin-biotin complex (Vector Labs) for 1 h. Sections were then washed and developed with diaminobenzidine substrate using the avidin-biotin horseradish peroxidase system (Vector Labs, Burlingame, CA, USA). Images were obtained with a digital Zeiss camera and analyzed using ImageJ. To quantify Ab pathology, images from 12 mice/group were taken with a Zeiss AxioImager A1 using a × 10 objective. Images were then merged to rebuild the whole slice. Merged images were analyzed using ImageJ and the percentage of area occupied by plaques was graphed.

Funding Information This work was supported by grants R01 AG037637 to S.O., from the Alzheimer's Drug Discovery Foundation to C.H., and from the Alzheimer's Drug Discovery Foundation and Harrington Discovery Institute to T.D.

Compliance with Ethical Standards Animal care and treatments were in accordance with the applicable regulation of the vivarium (The Institutional Animal Care and Use Committee of the Arizona State University).

References

1. Frautschy SA, Cole GM (2010) Why pleiotropic interventions are needed for Alzheimer's disease. Mol Neurobiol 41(2–3):392–409
2. Buccafusco JJ (2009) Multifunctional receptor-directed drugs for disorders of the central nervous system. Neurotherapeutics. 6(1):4–13
3. Cavalli A, Bolognesi ML, Minarini A, Rosini M, Tumiatti V, Recanatini M, Melchiorre C (2008) Multi-target-directed ligands to combat neurodegenerative diseases. J Med Chem 51(3):347–372
4. Weinreb O, Mandel S, Bar-Am O, Yogev-Falach M, Avramovich-Tirosh Y, Amit T, Youdim MBH (2009) Multifunctional neuroprotective derivatives of rasagiline as anti-Alzheimer's disease drugs. Neurotherapeutics. 6(1):163–174
5. Kimura R, Kamino K, Yamamoto M, Nuripa A, Kida T, Kazui H, Hashimoto R, Tanaka T et al (2007) The DYRK1A gene, encoded in chromosome 21 Down syndrome critical region, bridges between beta-amyloid production and tau phosphorylation in Alzheimer disease. Hum Mol Genet 16(1):15–23
6. Ryoo SR, Jeong HK, Radnaabazar C, Yoo JJ, Cho HJ, Lee HW, Kim IS, Cheon YH et al (2007) DYRK1A-mediated hyperphosphorylation of Tau. A functional link between Down syndrome and Alzheimer disease. J Biol Chem 282(48):34850–34857
7. Altafaj X, Dierssen M, Baamonde C, Marti E, Visa J, Guimera J et al (2001) Neurodevelopmental delay, motor abnormalities and cognitive deficits in transgenic mice overexpressing Dyrk1A (minibrain), a murine model of Down's syndrome. Hum Mol Genet 10(18):1915–1923
8. Ahn KJ, Jeong HK, Choi HS, Ryoo SR, Kim YJ, Goo JS, Choi SY, Han JS et al (2006) DYRK1A BAC transgenic mice show altered synaptic plasticity with learning and memory defects. Neurobiol Dis 22(3):463–472
9. Ferrer I, Barrachina M, Puig B, Martinez de Lagran M, Marti E, Avila J et al (2005) Constitutive Dyrk1A is abnormally expressed in Alzheimer disease, Down syndrome, Pick disease, and related transgenic models. Neurobiol Dis 20(2):392–400
10. Liu F, Liang Z, Wegiel J, Hwang YW, Iqbal K, Grundke-Iqbal I, Ramakrishna N, Gong CX (2008) Overexpression of Dyrk1A contributes to neurofibrillary degeneration in Down syndrome. FASEB J 22(9):3224–3233

11. Azorsa DO, Robeson RH, Frost D, Meec hoovet B, Brautigam GR, Dickey C et al (2010) High-content siRNA screening of the kinome identifies kinases involved in Alzheimer's disease-related tau hyperphosphorylation. BMC Genomics 11:25
12. Altafaj X, Martin ED, Ortiz-Abalia J, Valderrama A, Lao-Peregrin C, Dierssen M et al (2013) Normalization of Dyrk1A expression by AAV2/1-shDyrk1A attenuates hippocampal-dependent defects in the Ts65Dn mouse model of Down syndrome. Neurobiol Dis 52: 117–127
13. Pathak A, Rohilla A, Gupta T, Akhtar MJ, Haider MR, Sharma K, Haider K, Yar MS (2018) DYRK1A kinase inhibition with emphasis on neurodegeneration: a comprehensive evolution story-cum-perspective. Eur J Med Chem 158:559–592
14. Ryoo SR, Cho HJ, Lee HW, Jeong HK, Radnaabazar C, Kim YS, Kim MJ, Son MY et al (2008) Dual-specificity tyrosine(Y)-phosphorylation regulated kinase 1A-mediated phosphorylation of amyloid precursor protein: evidence for a functional link between Down syndrome and Alzheimer's disease. J Neurochem 104(5): 1333–1344
15. Kim EJ, Sung JY, Lee HJ, Rhim H, Hasegawa M, Iwatsubo T, Min DS, Kim J et al (2006) Dyrk1A phosphorylates alpha-synuclein and enhances intracellular inclusion formation. J Biol Chem 281(44): 33250–33257
16. Wegiel J, Dowjat K, Kaczmarski W, Kuchna I, Nowicki K, Frackowiak J, Mazur Kolecka B, Wegiel J et al (2008) The role of overexpressed DYRK1A protein in the early onset of neurofibrillary degeneration in Down syndrome. Acta Neuropathol 116(4):391–407
17. Becker W, Weber Y, Wetzel K, Eirmbter K, Tejedor FJ, Joost HG (1998) Sequence characteristics, subcellular localization, and substrate specificity of DYRK-related kinases, a novel family of dual specificity protein kinases. J Biol Chem 273(40):25893–25902
18. De la Torre R, De Sola S, Pons M, Duchon A, de Lagran MM, Farre M et al (2014) Epigallocatechin-3-gallate, a DYRK1A inhibitor, rescues cognitive deficits in Down syndrome mouse models and in humans. Mol Nutr Food Res 58(2):278–288
19. Branca C, Shaw DM, Belfiore R, Gokhale V, Shaw AY, Foley C, Smith B, Hulme C et al (2017) Dyrk1 inhibition improves Alzheimer's disease-like pathology. Aging Cell 16(5):1146–1154
20. Bierer LM, Hof PR, Purohit DP, Carlin L, Schmeidler J, Davis KL, Perl DP (1995) Neocortical neurofibrillary tangles correlate with dementia severity in Alzheimer's disease. Arch Neurol 52(1):81–88
21. Park J, Yang EJ, Yoon JH, Chung KC (2007) Dyrk1A overexpression in immortalized hippocampal cells produces the neuropathological features of Down syndrome. Mol Cell Neurosci 36(2):270–279
22. Wegiel J, Gong CX, Hwang YW (2011) The role of DYRK1A in neurodegenerative diseases. FEBS J 278(2):236–245
23. Jin M, Shepardson N, Yang T, Chen G, Walsh D, Selkoe DJ (2011) Soluble amyloid beta-protein dimers isolated from Alzheimer cortex directly induce tau hyperphosphorylation and neuritic degeneration. Proc Natl Acad Sci U S A 108(14):5819–5824
24. Zempel H, Thies E, Mandelkow E, Mandelkow EM (2010) Abeta oligomers cause localized Ca(2+) elevation, missorting of endogenous tau into dendrites, tau phosphorylation, and destruction of microtubules and spines. J Neurosci 30(36):11938–11950
25. Qi J, Zhang G (2019) Proteolysis-targeting chimeras for targeting protein for degradation. Future Med Chem 11:723–741
26. Frost D, Meechoovet B, Wang T, Gately S, Giorgetti M, Shcherbakova I, Dunckley T (2011) Beta-carboline compounds, including harmine, inhibit DYRK1A and tau phosphorylation at multiple Alzheimer's disease-related sites. PLoS One 6(5):e19264
27. Oddo S, Caccamo A, Kitazawa M, Tseng BP, LaFerla FM (2003) Amyloid deposition precedes tangle formation in a triple transgenic model of Alzheimer's disease. Neurobiol Aging 24(8):1063–1070
28. Becker W, Sippl W (2011) Activation, regulation, and inhibition of DYRK1A. FEBS J 278(2):246–256
29. Sonamoto R, Kii I, Koike Y, Sumida Y, Kato-Sumida T, Okuno Y, Hosoya T, Hagiwara M (2015) Identification of a DYRK1A inhibitor that induces degradation of the target kinase using co-chaperone CDC37 fused with luciferase nanoKAZ. Sci Rep 5:12728
30. Belfiore R, Rodin A, Ferreira E, Velazquez R, Branca C, Caccamo A et al (2019) Temporal and regional progression of Alzheimer's disease-like pathology in 3xTg-AD mice. Aging Cell 18(1):e12873
31. Woods YL, Cohen P, Becker W, Jakes R, Goedert M, Wang X et al (2001) The kinase DYRK phosphorylates protein-synthesis initiation factor eIF2Bepsilon at Ser539 and the microtubule-associated protein tau at Thr212: potential role for DYRK as a glycogen synthase kinase 3-priming kinase. Biochem J 355(Pt 3:609–615
32. Lai AY, McLaurin J (2012) Clearance of amyloid-beta peptides by microglia and macrophages: the issue of what, when and where. Future Neurol 7(2):165–176
33. Oddo S, Billings L, Kesslak JP, Cribbs DH, LaFerla FM (2004) Abeta immunotherapy leads to clearance of early, but not late, hyperphosphorylated tau aggregates via the proteasome. Neuron. 43(3):321–332
34. Beke L, Kig C, Linders JT, Boens S, Boeckx A, van Heerde E et al (2015) MELK-T1, a small-molecule inhibitor of protein kinase MELK, decreases DNA-damage tolerance in proliferating cancer cells. Biosci Rep 35(6):e00267
35. Gu S, Cui D, Chen X, Xiong X, Zhao Y (2018) PROTACs: an emerging targeting technique for protein degradation in drug discovery. Bioessays. 40(4):e1700247
36. Caccamo A, Medina DX, Oddo S (2013) Glucocorticoids exacerbate cognitive deficits in TDP-25 transgenic mice via a glutathione-mediated mechanism: implications for aging, stress and TDP-43 proteinopathies. J Neurosci 33(3):906–913
37. Branca C, Wisely EV, Hartman LK, Caccamo A, Oddo S (2014) Administration of a selective beta2 adrenergic receptor antagonist exacerbates neuropathology and cognitive deficits in a mouse model of Alzheimer's disease. Neurobiol Aging 35(12):2726–2735